Characterization of microparticles and oxide layers generated by laser irradiation of diamond-machined silicon wafers

2011 Semicond. Sci. Technol. 26 025006

(http://iopscience.iop.org/0268-1242/26/2/025006)

Semicond. Sci. Technol. **26** (2011) 025006 (7pp) doi:10.1088/0268-1242/26/2/025006

Characterization of microparticles and oxide layers generated by laser irradiation of diamond-machined silicon wafers

Jiwang Yan[1], Shin Sakai[2], Hiromichi Isogai[2] and Koji Izunome[2]

[1] Department of Nanomechanics, Graduate School of Engineering, Tohoku University, Aramaki Aoba 6-6-01, Aoba-ku, Sendai 980-8579, Japan
[2] Covalent Materials Corporation, 6-861-5 Higashiku, Seirou-machi, Kitakanbara-gun, Niigata 957-0197, Japan

E-mail: yanjw@pm.mech.tohoku.ac.jp

Received 13 July 2010, in final form 8 September 2010
Published 17 December 2010
Online at stacks.iop.org/SST/26/025006

Abstract
Nanosecond-pulsed laser irradiation is a potential method for removing machining-induced subsurface damage from silicon wafers. In this study, the material compositions and microstructures of microparticles and oxide layers generated during laser irradiation were investigated by atomic force microscopy, energy-dispersive x-ray spectroscopy, cross-sectional transmission electron microscopy, electron energy-loss spectroscopy and Auger electron spectroscopy. The oxide layer was found to be approximately 5 nm thick, which is significantly thicker than the native oxide layer of silicon at room temperature in air (∼1 nm). The microparticles have a low-density amorphous structure and are mainly composed of silicon oxide, while a few particles contain silicon. The particles are attached to the substrate, but are distinct from it. The results indicate that silicon boiled during the laser pulse and that the particles are recondensed and oxidized liquid silicon boiled away from the wafer surface. The microparticles can be completely removed from the wafer surface by hydrofluoric acid etching.

(Some figures in this article are in colour only in the electronic version)

1. Introduction

Abrasive machining processes, such as slicing, grinding, lapping and polishing, are widely employed in silicon wafer production. These machining processes generate subsurface damage, such as microstructural changes and dislocations, in silicon substrates [1–5]. It is essential to completely remove this damage to produce high-quality wafers. Chemical etching and chemo-mechanical polishing are currently used by the semiconductor industry to remove wafer damage. An alternative method that is currently being considered is laser irradiation. Yan *et al* [6] demonstrated the feasibility of recovering the lattice structure of a diamond-cut silicon wafer using nanosecond-pulsed Nd:YAG laser. This method has also been used to process silicon wafers machined by ultraprecision ductile-mode grinding [7]. It was confirmed that the grinding damage is completely removed and that grinding marks on the wafer surface are smoothed to a nanometer level. As laser irradiation is more rapid, cleaner, and less costly than conventional chemo-mechanical processes, it has considerable potential as an innovative post-machining process to improve the subsurface integrity of silicon wafers.

As shown in the previous paper [7], to achieve a completely subsurface damage-free wafer, the laser energy density must be increased to >0.72 J cm^{-2}, otherwise subsurface damage recovery will be incomplete. However, at high laser energy density (>1.04 J cm^{-2}), submicron particles appeared on the wafer surface after irradiation, which greatly increased the surface roughness. Therefore, particle generation at high laser power is a major obstacle to industrial application of the laser recovery technology.

Reasons for particle generation may include environmental contamination, contamination from the grinding process (i.e. from diamond abrasives or bonding

materials), recondensation of silicon boiled away from the wafer surface and material growth from the substrate during laser irradiation. To find possible solutions to prevent microparticle generation, it is critical to determine the particle generation mechanism.

Another aspect that should be clarified is the thickness of the oxide layer generated on silicon wafers by laser irradiation. Silicon wafers have native oxide layers that are ∼1 nm thick at room temperature and in air [8]. During laser irradiation, very high instantaneous temperatures (higher than the melting point of silicon, which is 1412 °C) are generated. Thus, a thick silicon oxide layer may form on the wafer surface after laser irradiation. However, no studies have investigated this aspect.

In this study, we employed several characterization methods to perform a detailed investigation of the material compositions and microstructures of the microparticles and the oxide layer. Based on the results, we discuss the particle generation mechanism and propose methods for eliminating particles.

2. Experimental procedures

Boron-doped *p*-type device-grade single-crystal silicon (1 0 0) wafers prepared by diamond grinding were used as samples. Grinding was performed using an ultraprecision grinder equipped with vitrified grinding wheels with diamond abrasives. The abrasive grains had an average size of approximately 2 μm. The machined samples were then irradiated with a Nd:YAG laser (QuikLaze-50, New Wave Research, Inc., Fremont, US). Details regarding the laser can be found in [6] and [7]. Single pulses with a pulse width of 3–4 ns were used. Two laser pulse energies were used, 4.16 and 5.76 μJ, which gave energy intensities of 1.04 and 1.44 J cm^{-2}, respectively. Microparticles should be generated on wafer surfaces under these conditions [7]. After laser irradiation, the surface topographies of the samples were examined by atomic force microscopy (AFM; Veeco, Nanoscope IIIa). AFM measurements were performed in a 3×3 μm^2 area in tapping mode.

Accurate characterization of the microstructures and compositions of microparticles is technologically difficult for any single characterization method due to the sensing limits and uncertainty. In this study, to obtain reliable results, we used multi-approach characterization. Firstly, energy-dispersive x-ray spectroscopy (EDX) analysis was performed using a Seiko SDI 4000 EDX system attached to a scanning electron microscope (SEM). The acceleration voltage of the SEM and EDX was 15 kV. The spot size of the electron beam used in the EDX analysis was 4 nm. Cross-sectional transmission electron microscopy (XTEM; Hitachi, H-9000UHRII; acceleration voltage: 300 kV) was used to measure the thicknesses of the oxide layers and to examine the structure of the interface between the microparticles and the substrate. The XTEM samples were thinned to approximately 100 nm using a dual-beam focused ion beam (FIB) system (FEI, Strata 400S). A thin layer of platinum (Pt) was deposited on the sample surface to mark the FIB position. A carbon (C) coating was deposited to protect the sample from possible damage during FIB sampling. Using the XTEM system, electron energy-loss spectroscopy (EELS) analysis was performed, where the nominal spot size of the electron beam was 0.7 nm. Finally, Auger electron spectroscopy (AES) analysis was performed by scanning Auger microscopy (Ulvac-Phi, 670; acceleration voltage: 10 kV; beam spot diameter: 50 nm). AES analysis was initially performed from the sample surface and subsequently from an interior region in the sample by removing a thin layer of material (thickness ∼10 nm) from the sample surface by argon (Ar) ion etching prior to performing AES analysis.

3. Results and discussion

3.1. AFM, SEM and EDX analyses

Figures 1(*a*) and (*b*) show AFM images of the wafer surface before and after laser irradiation at an energy density of 1.04 J cm^{-2}, respectively. Before laser irradiation, numerous parallel microgrooves are visible on the surface (figure 1(*a*)). The microgrooves are a few tens of nanometers high and several hundreds of nanometers wide, giving an arithmetic average surface roughness of 10 nmRa, while the maximum height of the surface profile was 117 nmRy. These microgrooves were formed through scratching by diamond abrasive grains during ductile-mode grinding. The microgrooves were significantly flattened after laser irradiation (figure 1(*b*)), although there were a few sharp protrusions on the surface. The protrusions range from a few tens of nanometers to several hundreds of nanometers in size. These protrusions caused the maximum height of the surface profile to increase to 121 nmRy, whereas the arithmetic average surface roughness decreased to 4 nmRa, which is considerably smaller than that in figure 1(*a*).

Figure 2 shows SEM micrographs of the same samples as those in figure 1. Microgrooves are clearly observable on the surface in figure 2(*a*). There are extremely small burrs and pile-ups of material on the sides of the grooves, indicating that the wafer surface was machined in a completely ductile mode (i.e. microscopic plastic flow of material dominated in the grinding process). The microgrooves disappeared after laser irradiation (figure 2(*b*)) and irregular-shaped microparticles of different sizes appeared on the surface. The largest particle (indicated by the red circle in figure 2(*b*)) is approximately 400 nm wide.

Figure 3 shows an EDX spectrum of the particle indicated by the red circle in figure 2(*b*). A very intense peak due to silicon (Si) is shown, whereas the peaks for other elements are negligible. As no other elements were detected, it is presumable that the particles are not contaminations from the environment or from the grinding process (i.e. from the diamond abrasive grains). It should be noted that the spectrum in figure 3 may contain a response from the substrate. Although the electron beam spot size was nominally 4 nm, the electron beam will be scattered considerably when it passes through the particle. The spatial resolution of EDX is estimated to be 1 μm or larger. Moreover, as an electron beam can penetrate to a depth of approximately 500 nm in silicon,

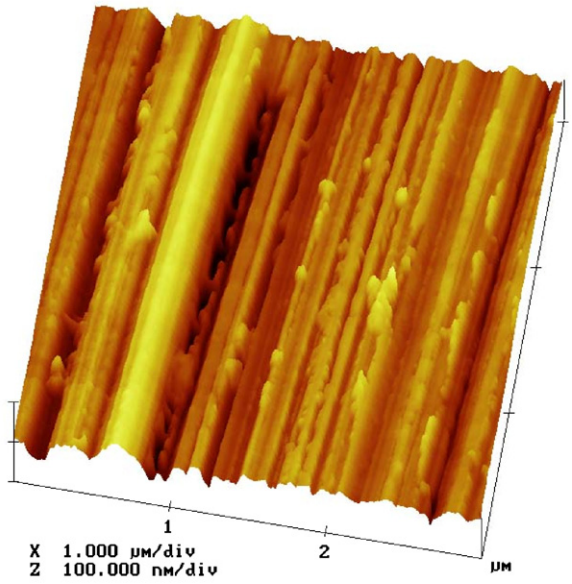

(*a*)

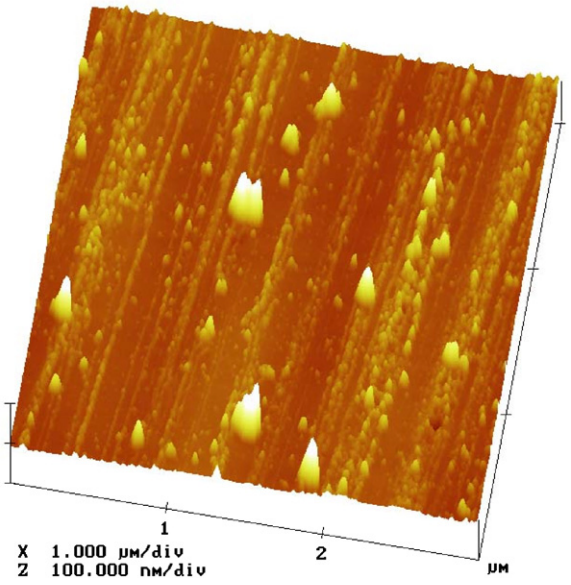

(*b*)

Figure 1. AFM images of the wafer surface: (*a*) before and (*b*) after laser irradiation at an energy density of 1.04 J cm^{-2}.

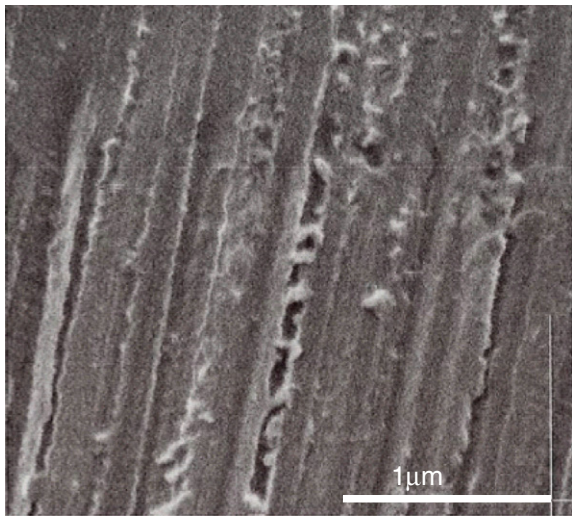

(*a*)

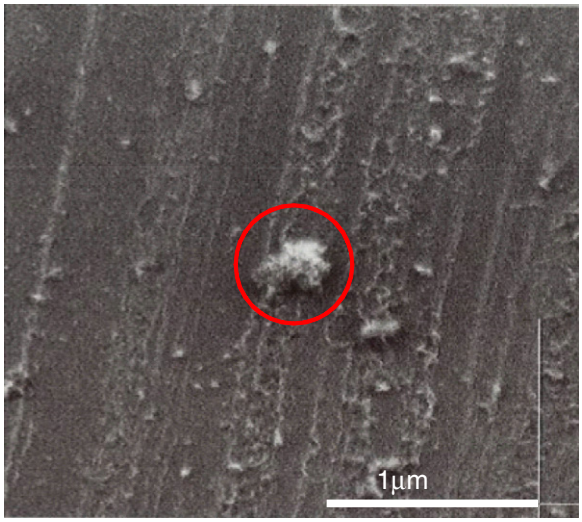

(*b*)

Figure 2. SEM micrographs of the same sample as that in figure 1 (*a*) before and (*b*) after laser irradiation.

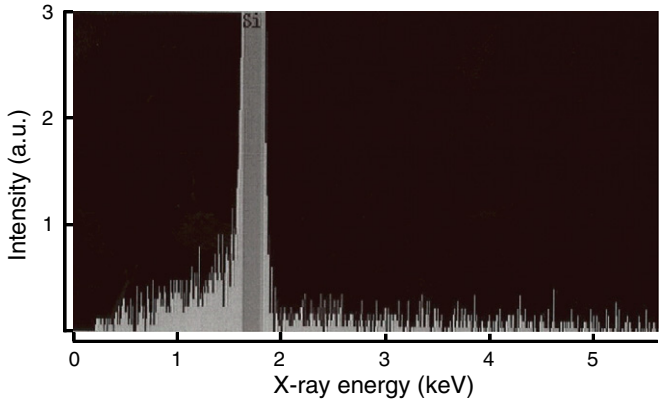

Figure 3. EDX spectrum of the particle indicated by the red circle in figure 2(*b*).

a response from deep within the substrate may be detected. Accounting for these considerations, the EDX spectrum in figure 3 does not exclude the possibility that the particle contains silicon oxide (SiO_2), but the oxygen (O) peak is too weak to be discriminated from the noise background on the left side of the Si peak in figure 3.

3.2. XTEM and EELS analyses

Figure 4 shows a bright-field XTEM micrograph of a particle formed on the wafer surface by laser irradiation at an energy density of 1.04 J cm^{-2}. The region enclosed by the dotted line is the particle and the dark region at the bottom is the single crystalline silicon (c-Si) substrate. The C protective coating (the light region around the particle) and the Pt marking layer (the black dots just beneath the C coating) can be clearly identified. Between the Pt layer and the c-Si substrate, there

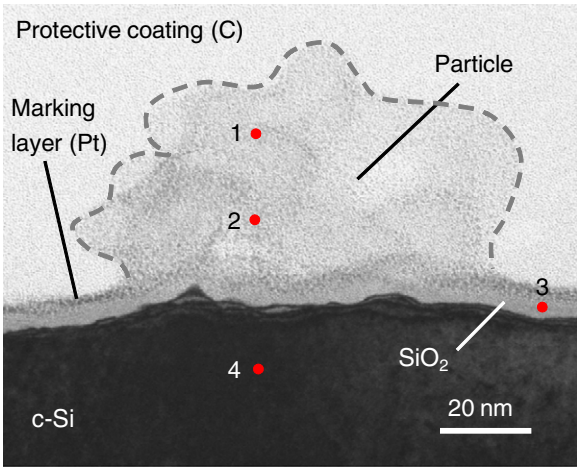

Figure 4. Bright-field XTEM micrograph of a microparticle formed on the wafer surface after laser irradiation at an energy density of 1.04 J cm^{-2}.

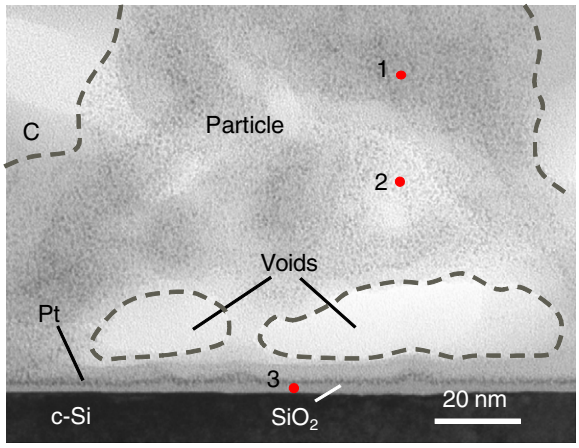

Figure 6. Bright-field XTEM micrograph of a microparticle formed on the wafer surface by laser irradiation at an energy density of 1.44 J cm^{-2}.

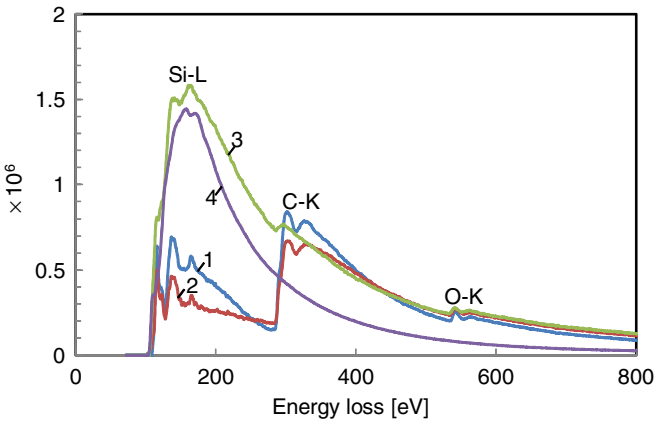

Figure 5. EELS spectra from points 1–4 in figure 4.

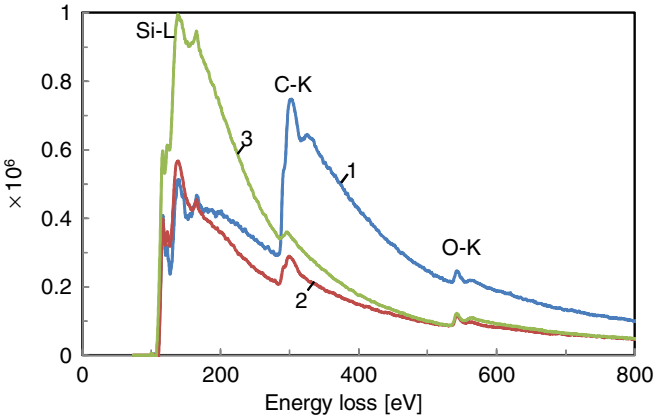

Figure 7. EELS spectra from points 1–3 in figure 6.

is a gray region, which presumably is the SiO_2 layer formed during laser irradiation. The contrast reveals that the particle has an amorphous structure and that the particle density is apparently lower than the density of the SiO_2 layer on the substrate. Pt dots are visible on the particle and on the particle–substrate interface. This indicates that the particle surface is far from smooth, but has many hollows and depressions, which results in a low-density structure. In addition, there are points where there is no contact between the particle and the substrate. In other words, the particle is attached to the substrate while being distinct from it.

Figure 5 shows EELS spectra obtained from the four points indicated by the numbers 1–4 in figure 4. Points 1 and 2 are located in the particle, point 3 is in the SiO_2 layer and point 4 is in the bulk of the substrate. The spectra from points 1 and 2 are very similar, with three intense peaks at the Si L , C K and O K edges. The peak at the C K edge is due to the C protective coating. By comparing the spectra in figure 5 with the reference spectra in [9], we found that the particle (points 1 and 2) is mainly composed of SiO_2 and that the spectrum from point 4 is due to Si. Unexpectedly, the spectrum from point 3 is due to a mixture of SiO_2 and Si; the reason for this has not been fully determined yet. Presumably, the response of Si in the spectrum from point 3 is from the substrate. Although the nominal beam spot size is 0.7 nm, the electron beam may be significantly scattered when it passes through the sample, which is 100 nm thick. Consequently, the response of the substrate is probably detected together with that of the SiO_2 layer.

Figure 6 shows a bright-field XTEM micrograph of another particle that was generated by laser irradiation at a higher energy density of 1.44 J cm^{-2}. The particle is bigger than the one in figure 4, but its microstructure and the particle–substrate interface are very similar to those in figure 4. There are two light regions at the bottom of the particle, which are presumably voids between the particle and the substrate. Figure 7 shows EELS spectra obtained from points 1–3 in figure 6. Similarly to the spectra in figure 5, the spectra from points 1 and 2 show peaks due to the Si L, C K and O K edges, indicating that the particle is mainly composed of SiO_2. The spectrum from point 3 contains a mixed response from Si and SiO_2.

Figure 8(*a*) shows a high-resolution multiple-wave interference XTEM micrograph of the interface between the particle and the substrate shown in figure 6. For comparison,

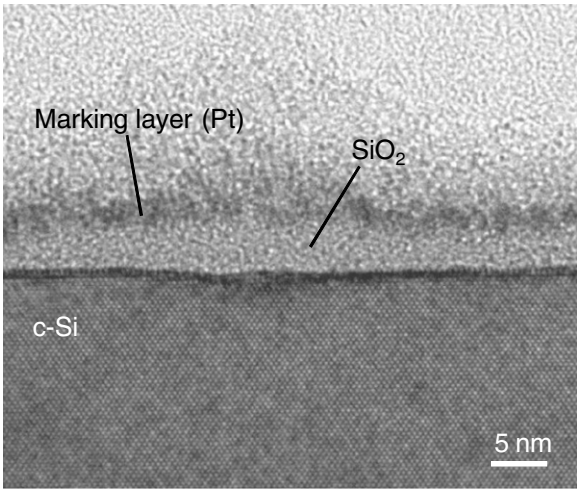

(*a*)

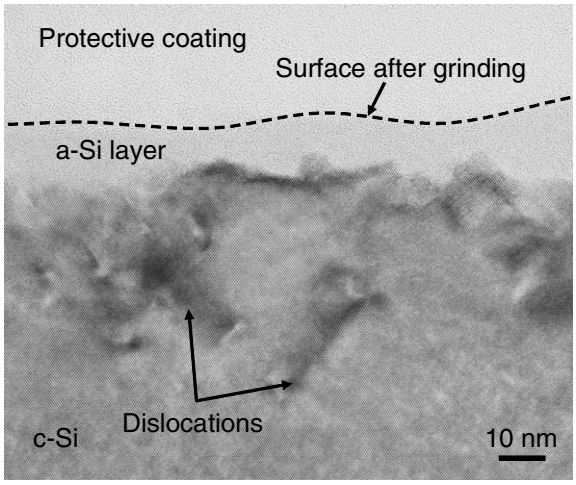

(*b*)

Figure 8. High-resolution multiple-wave interference XTEM micrographs of (*a*) the interface between the particle and the substrate shown in figure 6. (b) is an XTEM micrograph of the same wafer after diamond grinding but before laser irradiation.

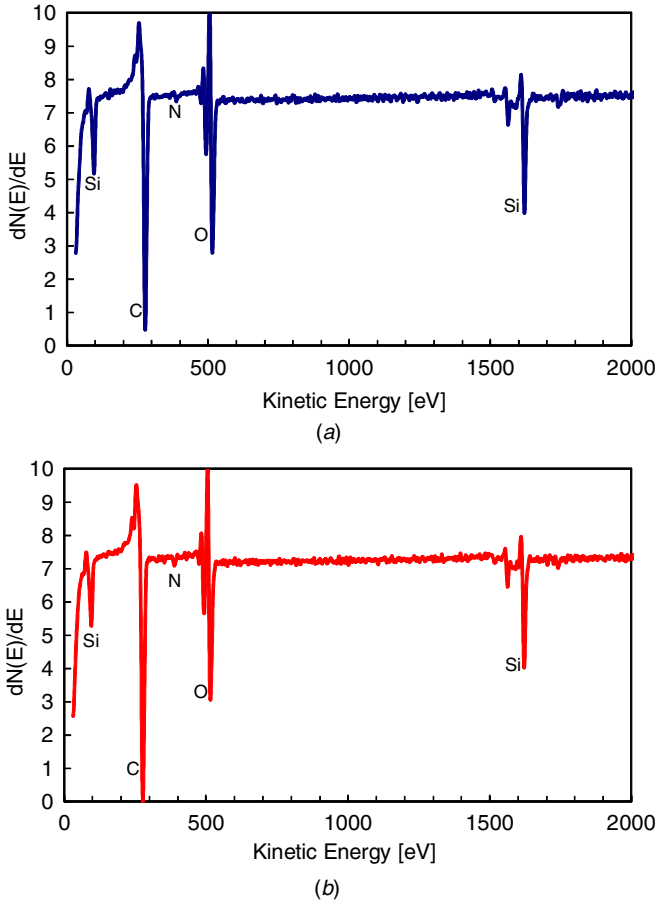

Figure 9. AES spectra of (*a*) a particle-free region of the silicon substrate and (*b*) a microparticle on the substrate prior to Ar-ion etching.

an XTEM micrograph of the same specimen before laser irradiation is shown in figure 8(*b*), where a grinding-induced amorphous silicon (a-Si) layer (thickness 10–20 nm) is seen, below which there are many dislocations. In figure 8(*a*), the lattice structure of single-crystal silicon can be clearly identified in the substrate, which strongly indicates that subsurface damage induced by grinding (as seen in figure 8(*b*)) has been completely removed by laser irradiation. The SiO_2 layer on the substrate is amorphous and has a denser structure than that in the particle. The SiO_2 layer is ∼5 nm thick, which is significantly thicker than the native oxide layer of silicon at room temperature in air (∼1 nm) [8]. As the oxide layer has uniform density and thickness, it may be possible to use laser irradiation to grow well-controlled SiO_2 layers on silicon, which has conventionally been realized by thermal oxidation at high temperatures (600–1200 °C) in air or other environments (e.g., O_2 or H_2O) [10]. That is to say, by laser irradiation, oxide layer growth can be realized concurrently with subsurface damage removal. This is under further investigation by examining the depth of silicon oxide under various laser power, pulse width/frequency and oxygen concentration in the environment.

By the way, it is noted that the oxide layer in figure 4 looks thicker than that in figure 6 (also figure 8(*a*)). This result looks inconsistent with the fact that the laser energy density used in figure 4 was lower than that in figure 6. This is because the TEM micrograph in figure 4 does not show exactly the real thickness of the oxide layer. As the laser irradiated surface is rough, the contrast of the oxide layer involves overlapped response from the wavy oxide layer in the thickness direction of the specimen (thickness 100 nm). For this reason, the oxide layer thickness observed from the cross section of the specimen looks bigger than its real thickness. In contrast, the TEM micrograph in figure 6 (also figure 8(*a*)) presents the real thickness of the oxide layer because the surface is very smooth in this case.

3.3. AES analysis

Figures 9(*a*) and (*b*) show AES spectra of a particle-free region of the silicon wafer and a microparticle on the wafer, respectively. As the sample had not been processed by Ar-ion

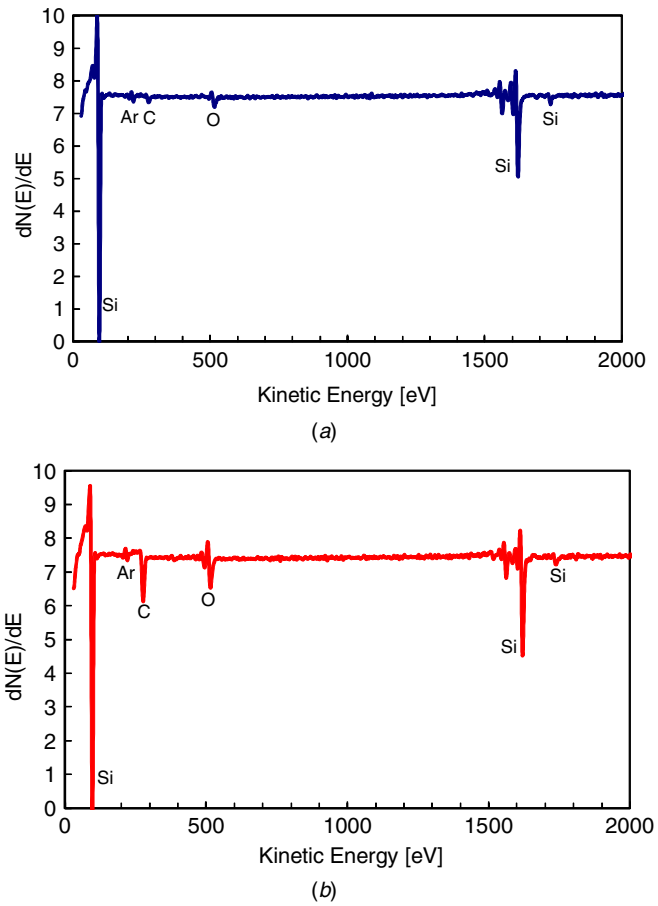

Figure 10. AES spectra of the same sample as that in figure 9 after it had been processed by Ar-ion etching: (*a*) substrate and (*b*) particle.

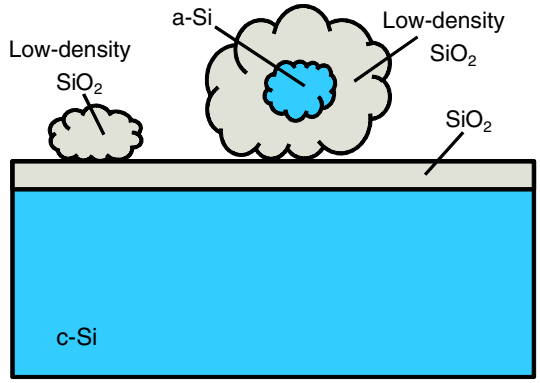

Figure 11. Schematic model of the laser-induced microparticles and oxide layer.

etching, the spectra in figure 9 are the responses mainly from the surfaces of the substrate and the particle. The two spectra are very similar, both showing strong responses at typical kinetic energies of Si, O and C [11]. These results indicate that both the particle and the wafer surface consist of SiO_2, though the composition ratio between Si and O obtained from the AES spectra shown in figure 9 is 1:1.2, higher than the stoicheiometric composition of SiO_2 (1:2). The particle has a loose structure, thus the Auger electrons are generated not only from particle surface (mainly SiO_2), but also from the dotted silicon grains in the particle, and from the silicon substrate below the particle. The peaks of C are due to the protective coating, and the peaks of nitrogen (N) in these spectra may be due to organic contamination from the environment prior to depositing C and Pt. Another possible reason of the N peaks might be nitridation of silicon during laser irradiation. As the laser irradiation tests were performed in air, the high temperature might have caused slight nitridation of silicon.

Figure 10 shows AES spectra of the same sample as that in figure 9 except that the sample had been processed by Ar-ion etching prior to AES analysis. In this case, the AES spectra were obtained mainly from within the substrate and particle. The response from the residual particle surface might also be detected because the Ar-ion etching could not remove completely the entire surface layer of a particle with irregular shape. In both figures 10(*a*) and (*b*), the Si peak is more intense than in figure 9, whereas the O peak intensity is considerably smaller. In particular, the O peak in figure 10(*a*) is almost nonexistent. This result demonstrates that the particle contains Si in the interior region and SiO_2 in the outside region.

3.4. Particle formation mechanism

The calculation in [7] revealed that the wafer surface temperature increases with increasing laser energy density. When the laser energy density is 0.96 J cm^{-2}, the wafer surface temperature is 3028 °C, which is higher than the boiling point of silicon (2878 °C) [12]. The results obtained in this study provide new evidence for silicon boiling. That is, silicon at the surface boils and forms small droplets. After the laser pulse finishes, these droplets resolidify and reattach to the surface. At the same time, both the substrate and particles are oxidized. As the droplets are recondensed and oxidized in free space, the resulting particles have a less dense structure than the SiO_2 film that forms on the substrate. In addition, oxidization may be incomplete in a few droplets, especially the bigger ones. In this case, silicon grains with amorphous structures may remain in the resulting particles. Figure 11 schematically depicts a structural model of the particles and oxide layer.

3.5. Particle removal

Particle generation can be prevented using a lower laser energy density (<0.96 J cm^{-2}) [7]. When this is done, silicon melts without boiling so that the subsurface damage is removed without forming unwanted particles. However, particles will be generated when high laser energy densities are required (e.g., to process wafers with deep damage and rough surfaces) and they must be removed by employing subsequent processes.

In this study, hydrofluoric (HF) acid etching was performed on samples with laser-generated particles. The etchant used was 1 wt% HF. The etching time was set to 20 min, which was estimated based on the etching rate (~0.1 nm s^{-1}) of thermally formed SiO_2 [8]. After etching, the samples were washed in flowing pure water for 5 min before SEM observations. Figures 12(*a*) and (*b*) show SEM micrographs

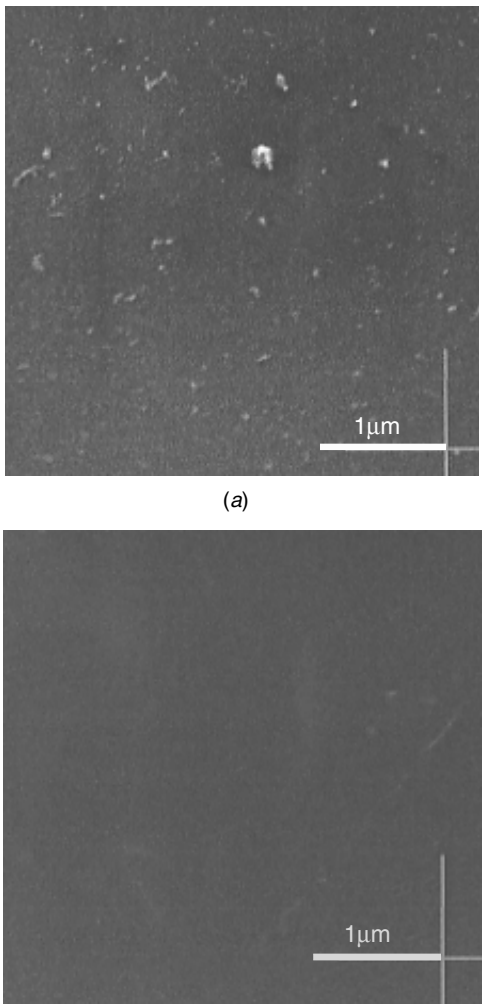

Figure 12. SEM micrographs of the wafer surface (*a*) before and (*b*) after HF etching.

of the wafer surface before and after HF etching, respectively. Prior to etching, numerous microparticles are visible on the wafer surface, whereas after etching, there are no particles and the surface is extremely smooth.

4. Conclusions

Microstructures and material compositions of microparticles and oxide layers formed by laser irradiation of diamond-machined silicon wafers were investigated by AFM, SEM-EDX, XTEM-EELS, and AES. The main conclusions are as follows.

(1) The oxide layers generated on silicon wafers by laser irradiation are ∼5 nm thick, which is significantly thicker than that of the native oxide layer on silicon at room temperature and in air (∼1 nm). It may be possible to grow well-controlled SiO_2 layers on silicon concurrently with the subsurface damage removal.
(2) The microparticles have submicron dimensions and irregular shapes. They are attached to the substrate, but are distinct from it.
(3) The microparticles are mainly composed of SiO_2. A few particles also contain silicon in the interior regions. The particles have a less dense structure than the SiO_2 layer on the substrate.
(4) The microparticles are formed by resolidification and oxidation of liquid silicon boiled away from the wafer surface during laser irradiation.
(5) The microparticles can be completely removed by HF etching.

Acknowledgments

This work was supported in part by a grant-in-Aid for Exploratory Research (project no 20656023) from the Japan Society for the Promotion of Science (JSPS).

References

[1] Shibata T, Ono A, Kurihara K, Makino E and Ikeda M 1994 *Appl. Phys. Lett.* **65** 2553–5
[2] Puttick K E, Whitmore L C, Chao C L and Gee A E 1994 *Phil. Mag.* A **69** 91–103
[3] Gogotsi Y, Baek C and Kirscht F 1999 *Semicond. Sci. Technol.* **14** 936–44
[4] Yan J 2004 *J. Appl. Phys.* **95** 2094–101
[5] Yan J, Asami T and Kuriyagawa T 2007 *Precis. Eng.* **32** 186–95
[6] Yan J, Asami T and Kuriyagawa T 2007 *Semicond. Sci. Technol.* **22** 392–5
[7] Yan J, Sakai S, Isogai H and Izunome K 2009 *Semicond. Sci. Technol.* **24** 105018
[8] Zhang X 2001 *Electrochemistry of Silicon and Its Oxide* (New York: Kluwer/Plenum)
[9] Ahn C C 2004 *Transmission Electron Energy Loss Spectrometry in Materials Science and the EELS ATLAS* (New York: Wiley-VCH)
[10] Lee S 2006 *Encyclopedia of Chemical Processing* (Boca Raton, FL: CRC Press)
[11] Davis L E, MacDonald N C, Palmberg P W, Riach G E and Weber R E 1976 *Handbook of Auger Electron Spectroscopy* (Eden Prairie, MN: Physical Electronics Industries)
[12] Yaws C L, Lutwack R, Dickens L L and Hsu G 1981 *Solid State Technol.* **24** 87–92